

Experimental report of EC948

M. Kobchenko, F. Renard, D. K. Dysthe

1. Overview

During the imaging campaign in 2012 at ESRF ID19, Grenoble, France in total 20 rock samples were imaged (**Appendix 1**). The cores were from a number of geological settings in Europe, South Africa and the US. The main purpose was to analyze the microstructure of samples under study and the porosity evolution during diagenesis. 2 samples of andesite (AND and ANDALT) were imaged to study how weathering process affects the internal structure of the rock. 8 of the samples were organic-rich shales (Green River Shales-GRS and Karoo shales-DP). They were exposed to gradual rising temperature under atmospheric pressure in the AET-oven while imaged with X-rays CT. A multi-resolution approach was applied to capture 3D volumes with 2.8 and 0.56 μm voxel size. This report will start with a brief summary of each experiment, continues with a review of the samples imaged and the obtained results and publications.

2. CT on the rock samples: andesite (AND and ANDALT)

This study was dedicated to processes operating during magma solidification and cooling. The pore structure of two samples, obtained from an andesitic sill intrusion, was determined by multi-scale resolution technique at 2.8 and 0.56 μm and the 3D data were used for transport modeling (**Figure 1**). Unaltered andesite has a power law distribution of pore volumes over a range of five orders of magnitude. The probability distribution function (PDF) scales with the inverse square of the pore volume (V). This scaling behavior is attributed to the coalescence of pores at crystal–melt boundaries. One scientific paper was published on these results in Earth and Planetary Science Letters (**Papers: 1**).

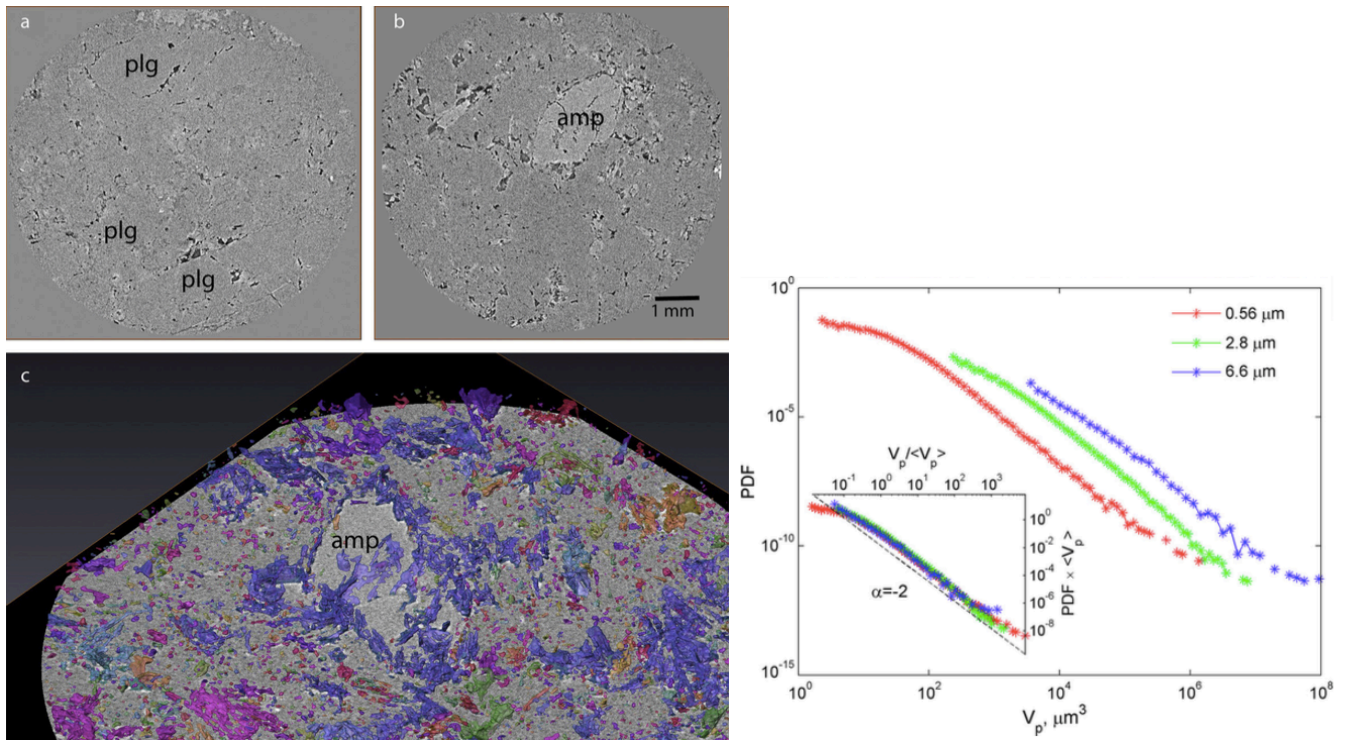


Figure 1: Left. a), (b) Original gray-level X-ray images of the rock matrix, 2D slices perpendicular to the axis of the sample cylinder (7 mm in diameter) shows the contrast between pores (black) and minerals (grey). (c) Clusters of connected porosity in a $\sim 300 \mu\text{m}$ Right. Pore volume probability distribution function (PDF) measured from 3D X- ray images obtained with three spatial resolutions (0.56, 2.8 and 6.6 μm voxel sizes). Inset: Data collapse of the pore volume distributions rescaled by their mean values at different pixel resolutions. The dashed line corresponds to a power-law ($\text{PDF}(V) \propto V^\alpha$, with $\alpha = -2$).

3. CT on the rock samples: organic-rich shales (GRS and Karoo)

In total 14 immature organic-rich shale samples (Karoo basin, South Africa which are denoted by “DP” and Green River Basin Shales, Utah represented by “GRS”) were heated and imaged with multi-resolutions setup at 2.8 and 0.56 μm .

Three experiments implying in-situ imaging during heating were conducted:

- 1) Three cores of 7 mm diameter were heated fast under atmospheric pressure in the oven at three different temperatures **390C, 335C and 290C** - **GRS_dot_II_npc1, GRS_dot_II_npc2, GRS_dot_II_npc4**. 3D images were acquired before heating, during heating and an overview of the whole core after heating (**Figure 3 A, B and C**). Depending on temperature different fracture patterns were observed (**Figure 2**). The higher was the temperature the denser crack network was formed. This data indicate interplay between rate of diffusion of produced hydrocarbons through the shale matrix to the fracture and the rate of organic matter maturation. These results can be used to predict the density of naturally formed fractures in an unconventional shale reservoir depending on the burial and heating history. **We have presented this material at two international conferences. We plan to write a scientific publication on this topic.**
- 2) Two cores of 7 mm and 2 mm diameter were placed in non-porous ceramic tubes and sealed from both ends with metal rods. They were gradually heated in the oven from 50 to 800C during 10-14 hours (**Figure 2, Right**). The sample **GRS_dot_VI_2_heat**, a core of 2 mm in diameter was imaged during heating from 50 to 750C and 75 scans were captured at 0.7 micron resolution. A porosity network can be detected in all images from the sequence (**Figure 4**). More detailed overview of this image sequence is provided further in the report. **We have presented this material at two international conferences. We prepare a scientific publication on this topic.** The sample **GRS_dot_II_npc3**, a 7 mm diameter core, was heated from 50 to 750C and imaged using multi-resolution technique at 2.8 and 0.56 μm . 22 scans were acquired at each resolution (44 scans in total). At the end of the experiment the confining ceramic cell was broken (**Figure 5**). At some moment during heating sequence the center of rotation of CT was moved and 80% of the scans were featured artifacts (**Figure 5**). Unfortunately this could not be corrected and these data were lost for subsequent analysis.
- 3) Two DP (Karoo) samples were heated at 290 C. One sample was confined in ceramic tube and metallic rods; another was heated under atmospheric pressure. Images of 2.8 and 0.56 μm resolution were acquired before heating, while heating and an overview of the whole sample was made after heating was complete (**Figure 6**). The porosity structure, crack geometry and shape differ dramatically from the ones observed in GRS samples.

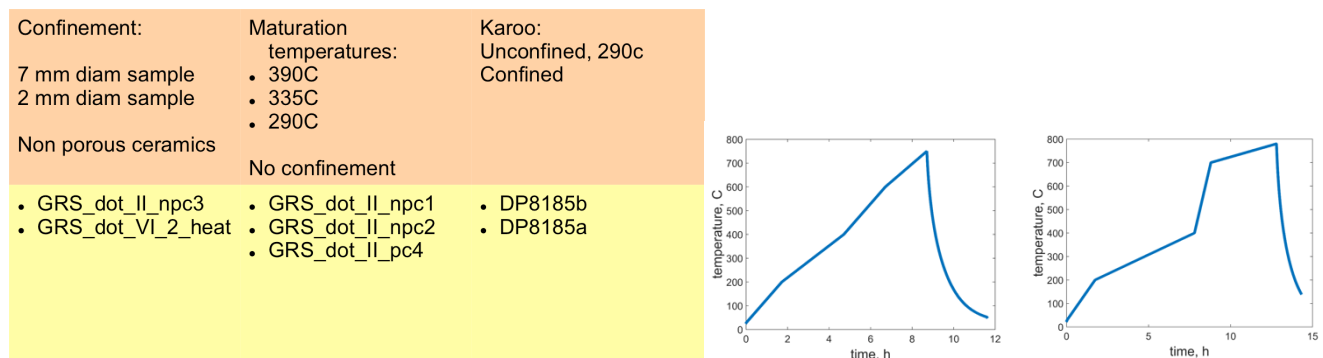


Figure 2: Left: Overview of heating experiments. **Right:** Graphs of the temperature variations during heating ramps used for gradual maturation of the samples GRS_dot_VI_2_heat and GRS_dot_II_npc3.

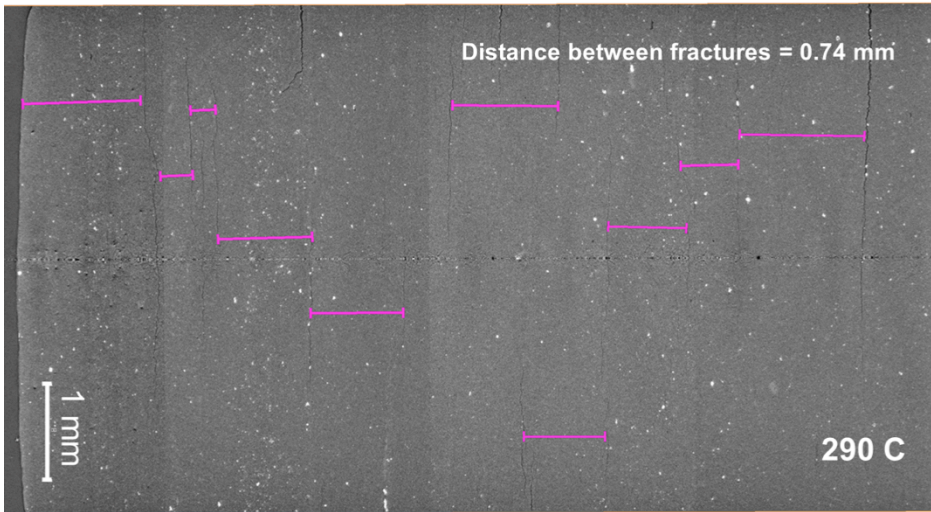


Figure 3A: Fracture network in the sample GRS_dot_II_pc4 after heating at 290C.

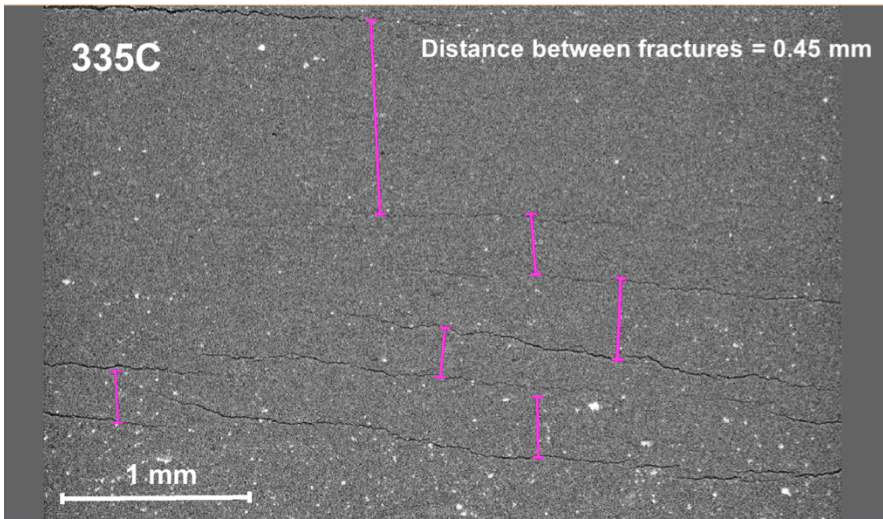


Figure 3B: Fracture network in the sample GRS_dot_II_npc2 after heating at 335C.

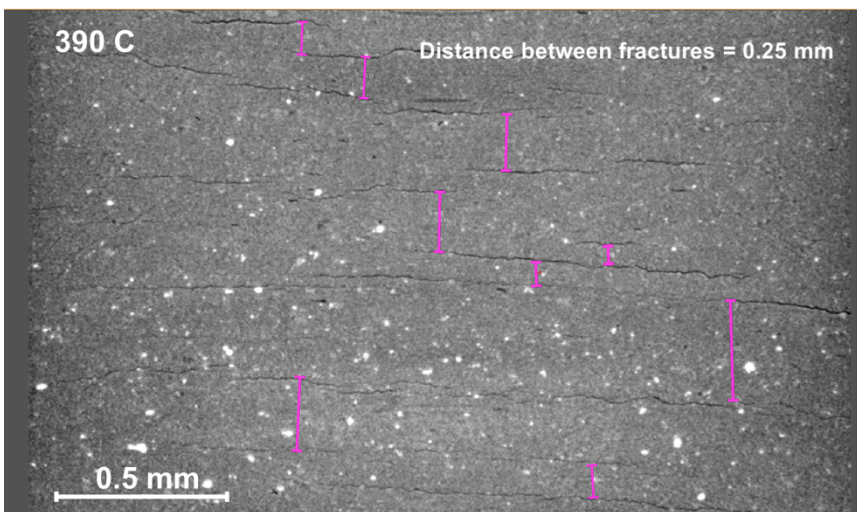
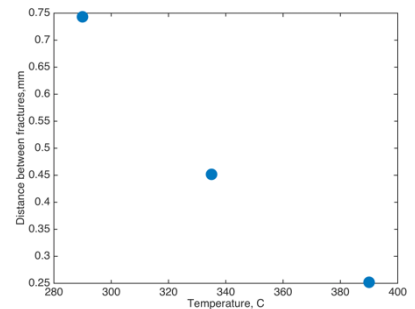


Figure 3C: Fracture network in the sample GRS_dot_II_npc1 after heating at 390C. Right: Crack network density in dependence of temperature for the three samples.



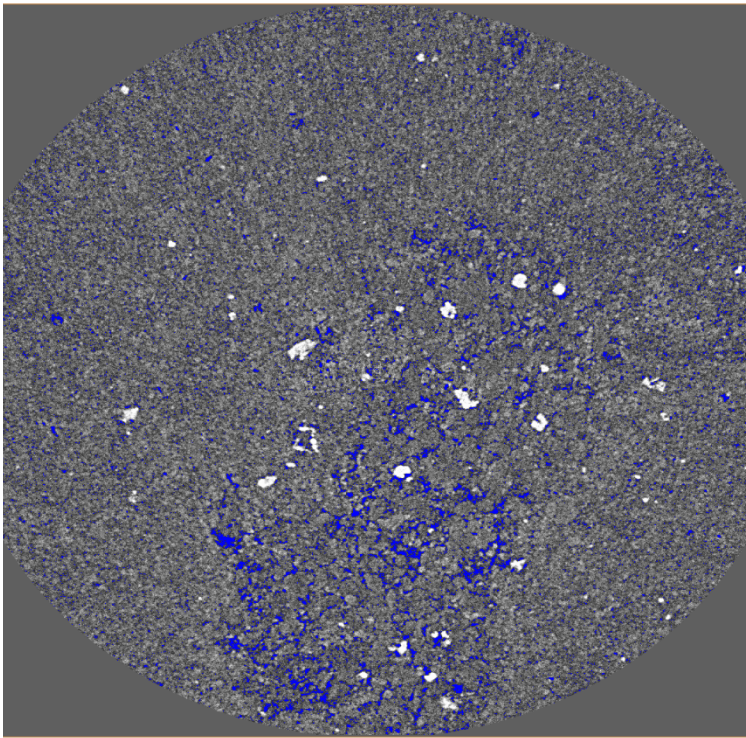


Figure 4: Porosity and fracture network indicated in blue was observed in the sample GRS_dot_VI_2_heat.

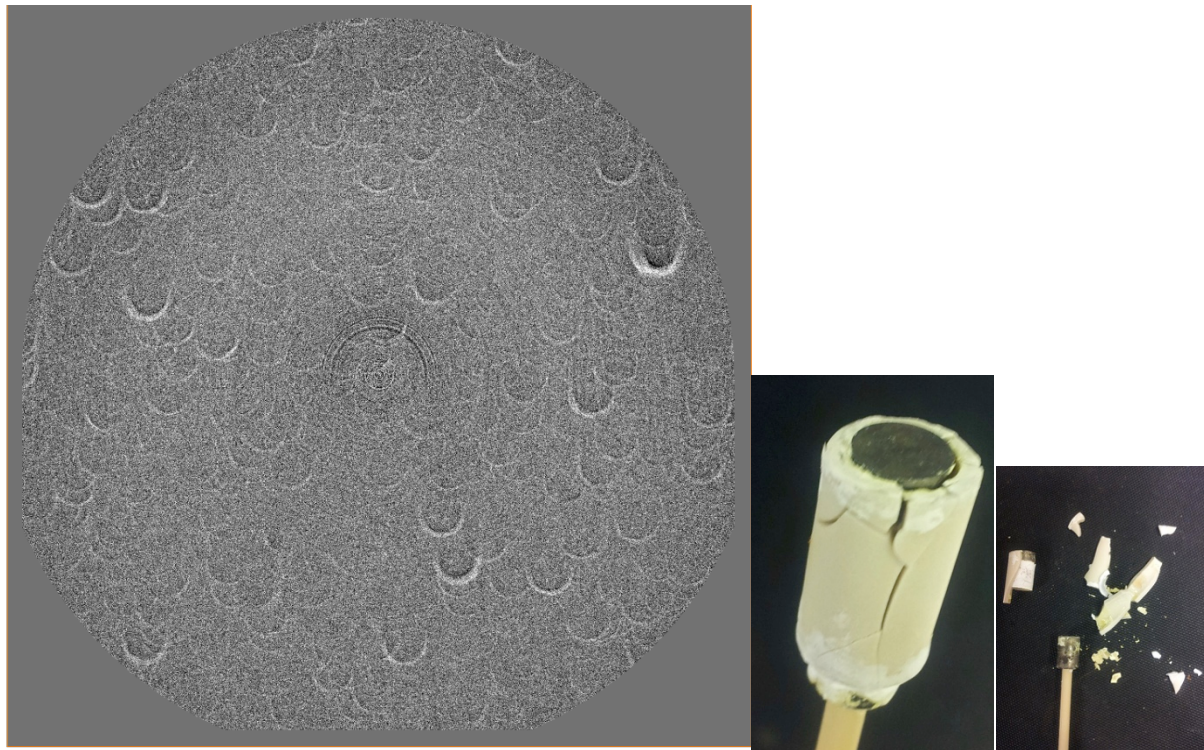


Figure 5: Images of the sample GRS_dot_II_npc3, the center of rotation was moved during acquisition and 80% of the data from the heating sequence feature such artifacts. **Right:** The confining ceramic cell was broken after heating.

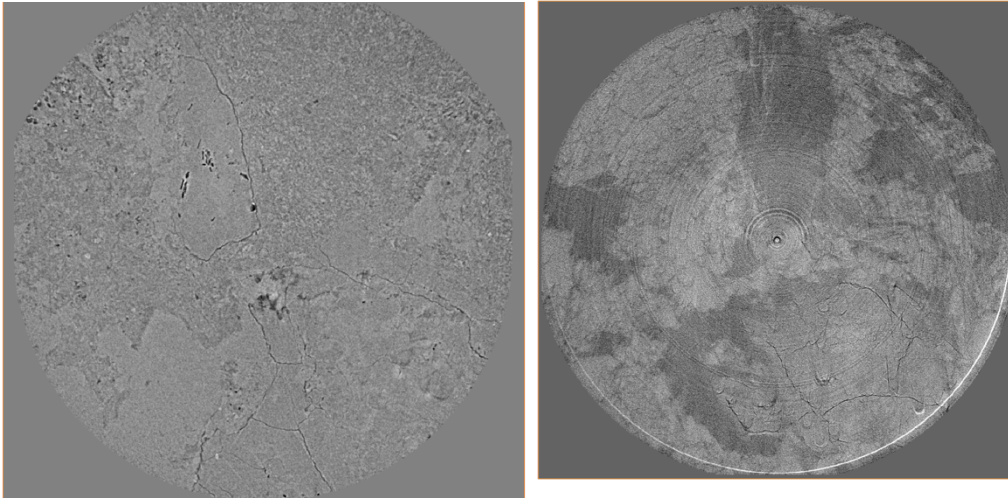


Figure 6: Images of DP samples at 2.8 and 0.56 μm . The pore structure and geometry of the fracture network is different from the ones observed in GRS samples.

4. Porosity evolution in the sample GRS_dot_VI_2_heat

During the heating from 50C to 750C dynamics of pore structure evolution in the sample GRS_dot_VI_2_heat evolution was observed. 75 volume of 1900x1900x1000 size (0.7 μm voxel size) were obtained at the rate 8 min per scan. The volumes represent a 0.7 mm field of view in the middle of the sample, however the boundaries are not visible. The image sequence was analyzed using Avizo software and Matlab. TCL codes were written to apply the developed image analysis workflow to the entire image series. Images were filtered, thresholded and labeled (**Figure 7**). A set of measurements was applied to characterize the porosity evolution with time. The variation of total porosity (volume of all pores in relation to the sample volume) indicates regime of fracture opening and closing (**Figure 8**).

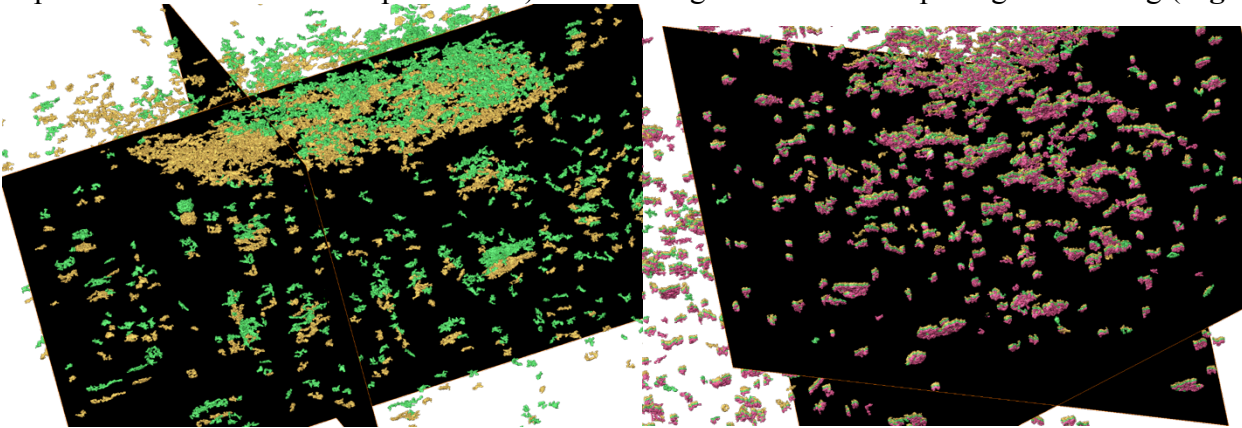


Figure 7: Overlapped labeled images of porosity structure in two subsequent volumes of GRS_dot_VI_2_heat.

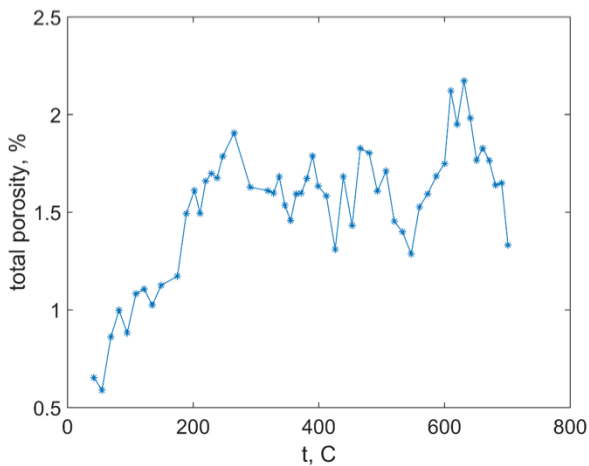


Figure 8: Variation of total porosity in the GRS_dot_VI_2_heat sample with time.

5. Commercial campaign in June 22nd, 2015 at ESRF ID19.

The purpose of this experiment was to acquire images of immature organic-rich GRS shale sample at 0.16 μm resolution. This sample was never imaged before with such high quality (**Figure 9**). This technique enabled to see the micro grains of the shale matrix mixed with organic material (**Figure 10 A, B**). Separate kerogen patches are clearly resolved and their shape is reconstructed in 3D (**Figure 10 C, D**). This data provide very valuable contribution to the understanding of the shale composition and proves that this experimental technique can be used to investigate how organic material evolves during heating and how micro-cracks originate from the kerogen lenses. We will use this result to propose a future experiment at ESRF ID19.

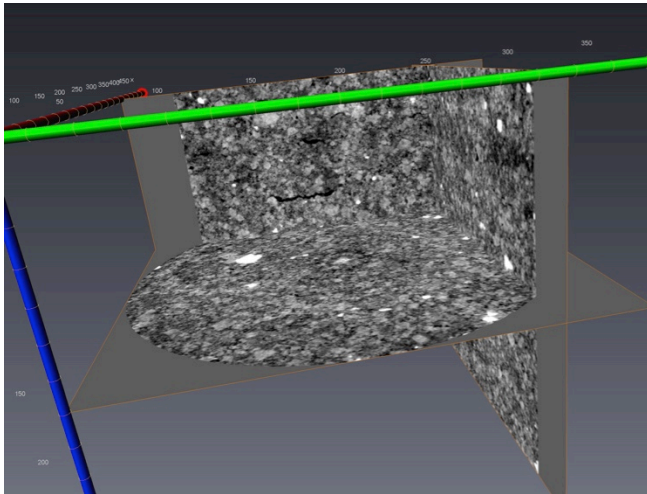


Figure 9: A 3D image of immature GRS sample at 0.16 μm resolution.

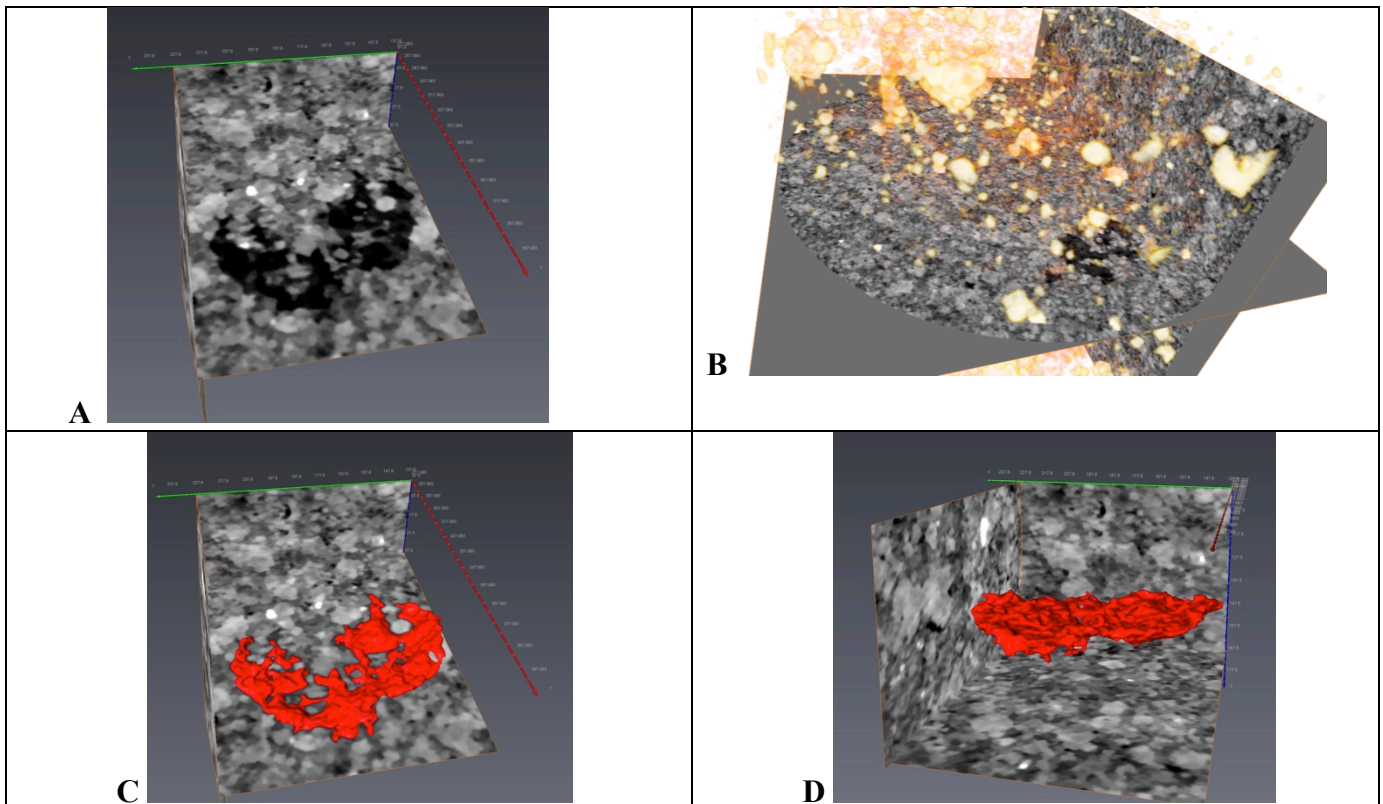


Figure 10: Mineral grains of the shale matrix with irregularly shaped kerogen lenses. C, D – reconstructed 3D shape of a kerogen patch.

Papers in international journals:

1) B. Jamtveit, M. Krotkiewski, **M. Kobchenko**, F. Renard and L. Angheluta; Pore-space distribution and transport properties of an andesitic intrusion. Earth and Planetary Science Letters, 2014.

Presentation at international conferences:

- 1) **M. Kobchenko**, D. K. Dysthe, F. Renard, B. Jamtveit, and A. Malthe-Sørenssen; Reaction-induced fracturing of low permeability solids; European Geophysical Union Fall Meeting, EGU 2015, April 2015.
- 2) **M. Kobchenko**, A. Pluymakers, D. K. Dysthe, F. Renard, and A. Malthe-Sørenssen; Simulation of hydrocarbon primary migration: multi-experimental approach; 11th Euro conference on rock physics and geomechanics; September 2015

Appendix 1: List of the scanned samples

sample	comment	Sample OD	3D raw
AND	andesite (Bjørn)	7 mm	2.8 µm and 0.56 µm-FTM 1000x2048 (Multiresseq macro)
ANDALT	altered Andesite (Bjørn)	7 mm	2.8 µm and 0.56 µm-FTM 1000x2048 (Multiresseq macro)
ROR1	Oliver Plumber's sample	2 mm	0.56 micron (Fasttomo macro)
ROR2	Oliver Plumber's sample	2 mm	0.56 micron (Fasttomo macro)
ETLAT08_4II1B	Oliver Plumber's sample	7 mm	2.8 micron and 0.56 micron-FTM 1000x2048 (Multiresseq macro)
ETCL_8_4	Oliver Plumber's sample	2 mm	0.56 micron (Fasttomo macro)
AUS1	Oliver Plumber's sample	7 mm	2.8 micron and 0.56 micron-FTM 1000x2048 (Multiresseq macro)
323_5	Maya's friend Sandstone	7 mm	2.8 µm and 0.56µm
343_10	Maya's friend Sandstone	7 mm	2.8 micron and 0.56 micron-FTM 1000x2048 (Multiresseq macro)
210_B	Maya's friend Sandstone	7 mm	2.8 µm and 0.56µm
31	Maya's friend Sandstone	7 mm	2.8 micron and 0.56 micron-FTM 1000x2048 (Multiresseq macro)
IND1(Fracture_Francois_2x)	Gratier Experiment	6 mm	2.8 micron (Fasttomo micro)
GRS_dot_IL_npc1	Green River Shale- unconfined	7 mm	2.8 micron-fast heated to 390 deg C and stayed for 2 hours-6 scans in total and 4 separate regional scans(a,b,c &d) at the end (out of the furnace)
GRS_dot_IL_npc2	Green River Shale-unconfined	7 mm	before heating 0.56micron and 2.8 micron, fast heating 335C 5 scans, after heating zoom at 0.56µm the same area, remove oven and take overview a,b,c at 2.8µm
GRS_dot_IL_npc3	Green River Shale-Non porous ceramic(10A 7x10 mm)	7 mm	Confined ID19-2.8 micron and 0.56 micron (22 scans per resolution)-heating various ramps to 780 deg. C-1900x1900x1000-2000 and 3000 radiographs (insitutomomultires), GRS_dot_IL_npc3.txt showing the temperature profile.
GRS_dot_IL_npc5	Green River Shale-Non porous ceramic(10A 7x10 mm)	7 mm	ID19-3.5 µm and 0,7 micron-1500 radiographs-18% transmission (2048x1900 pixels)-180°x10 done
GRS_dot_VI_2	Green River Shale-Non porous ceramic(10A 2x4 mm)	2 mm	Confined ID19-0.7 µm (1900x1900 pixels)-38% transmission-180°rotation--heating various ramps to 750 deg. C-2000 s (insitumultires), GRS_dot_VI_2_heat.txt showing the temperature profile.
GRS_dot_IL_pc4	Green River Shale-unconfined	7 mm	before heating 0.56micron and 2.8 micron, fast heating 290C 5 scans, after heating zoom at 0.56µm the same area, remove oven and take overview a,b,c,d at 2.8µm
DP8185b	Karoo unconfined		7 before heating 0,56 and 2,8 micron, heating at 290c 2,8 micron; after heating 0,56 and 2,8 micron for ob'erview
DP8185a	Karoo confined		7 before heating 0,56 and 2,8 micron, heating at 290c 2,8 micron; after heating 0,56 and 2,8 micron for ob'erview